Diffusive Propagation of Chemical Waves through a Microgap

Kenji Suzuki,* Tatsuo Yoshinobu, and Hiroshi Iwasaki

The Institute of Scientific and Industrial Research, Osaka University, 8−1 Mihogaoka, Ibaraki, Osaka 567-0047, Japan

Received: January 4, 2000; In Final Form: February 28, 2000

A photolithographic method was developed for micropatterning of catalyst (ferroin) for the Belousov−Zhabotinsky (BZ) reaction on a cation-exchange membrane. The propagation of chemical waves through microgaps on a catalyst line was quantitatively investigated. When a periodic train of chemical waves entered a microgap, the frequency of the chemical waves was converted into lower frequencies such as $^1/_2$, $^1/_3$, and $^1/_4$ of the original frequency depending on the gap width. The firing number depended on the gap width and the original frequency of the chemical waves. The frequency conversion is explained in terms of the recovery time of the BZ reaction media.

Introduction

Studies on the chemical waves in the Belousov−Zhabotinsky (BZ) reaction media have contributed to the understanding of waves in chemical and biological excitable systems.[1−6] Experiments on the chemical waves have been performed mainly in homogeneous aqueous solutions. On the other hand, biological systems are extremely inhomogeneous and have spatial structures. Recently, investigations on chemical waves in the presence of various inhomogeneities became active in order to provide some insights into the spatiotemporal pattern formations in biological systems.[7−16]

In many of the inhomogeneous BZ reaction media, the propagation of the chemical waves through a narrow gap, i.e., a catalyst-less zone, is one of the most essential phenomena for pattern formations of the chemical waves. DeSimone, Beil, and Scriven reported, in their pioneering work in 1973, on the propagation and the propagation failure of chemical waves through narrow slits in a membrane.[17] Linde and Zirkel have reported the frequency change of chemical waves at narrow splits of gel matrix.[18] Agladze, Dupont, and Krinsky have reported the drift of a spiral wave along a widening split of a polysulfone membrane.[19] These dynamics of the chemical wave in the presence of the narrow gap have been considered to be an important subject because of their similarity to those of waves in hearts.[20] In addition, even devices for chemical-based computation have been recently proposed, taking advantage of the narrow gaps in BZ reaction media[21−23] in order to explore the possibilities of information processing by excitable media. Most of the studies, however, have largely relied on numerical simulations, because of the experimental difficulty for microgaps of well-controlled gap widths. Thus the chemical wave propagation through the narrow gap have not been investigated quantitatively.

We report here a new technique to fabricate microgaps of ferroin patterns on a cation-exchange membrane. The system of this experiment is similar to that described by Steibock, Kettunen, and Showalter,[10] in which the patterns of the catalyst were formed on a cation-exchange membrane by an ink-jet printer. To fabricate catalyst patterns with microgaps precisely, we have employed a photolithographic technique, which we reported previously.[24] The aim of this paper is to clarify the basic properties of the propagation of the chemical waves through the microgaps.

Experimental Section

Fabrication of Catalyst Micropatterns. Figure 1 shows the photolithographic process employed in this study. A cation-exchange membrane of 0.18 mm in thickness (Dupont Nafion 117 perfluorosulfonic acid membrane) was immersed in hot water at 90 °C for 1 h and was fixed on a glass plate by silicone rubber (Shin-Etsu Chemical Co., Ltd., 1Component RTV KE45). A positive G-line photoresist (Shipley Far East S1818) was spin-coated onto the membrane. The membrane was covered with a mask, on which the desired pattern is printed, during exposure to the light from a mercury lamp. Then, the membrane was immersed in a developer (Shipley Far East MF-CD26) and rinsed in deionized water. Thereafter, it was immersed in an aqueous solution ([ferroin] = 12.5 mM, [ethanol] = 16 M) for 45 s to immobilize ferroin which functions as a catalyst in the BZ reaction. The ferroin molecules $[Fe(phen)_3]^{2+}$ are bonded to sulfonate groups ($-SO^{3-}$) in the membrane via Coulomb interaction. The photoresist on the membrane was removed by ethanol. The membrane was immersed in deionized water for 24 h in order to remove the ethanol and another contaminants. Then the membrane was immersed in an aqueous solution ($[H_2SO_4]$ = 1.5 M, $[NaBrO_3]$ = 1 M) for 3 h in order to decompose the ethanol left in the membrane by the oxidation reaction of ethanol with bromate. During the latter half of the immersion process, the color of the catalyst pattern turned from red to blue as a result of oxidation reaction of ferroin with bromate and this is the sign of the end of the oxidation process of ethanol. The membrane was rinsed in deionized water and stored in an aqueous solution ($[H_2SO_4]$ = 0.1 M). The color of the catalyst patterns gradually returns from blue to red.

Characterization of Catalyst Micropatterns. Figure 2a shows a ferroin pattern immobilized on the cation-exchange membrane, which is glued on a glass support by the silicone rubber. Ferroin is immobilized in the black area that looks like a comb pattern, and there is no ferroin in the white area. The comb pattern has 11 vertical lines (A)−(K) extending from the horizontal line, and each vertical line has a gap, a zone without

* Corresponding author. E-mail: Kenji31@sanken.osaka-u.ac.jp.

10.1021/jp000009n CCC: $19.00
Published on Web 05/04/2000

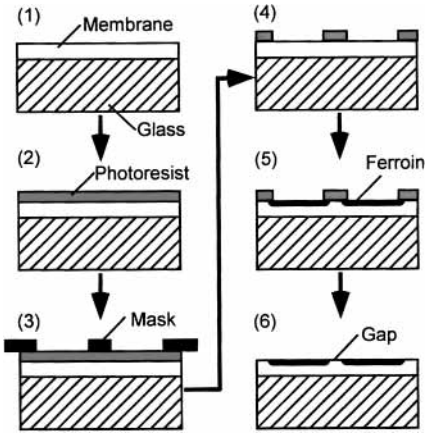

Figure 1. The process sequence of the catalyst patterning on the cation-exchange membrane.

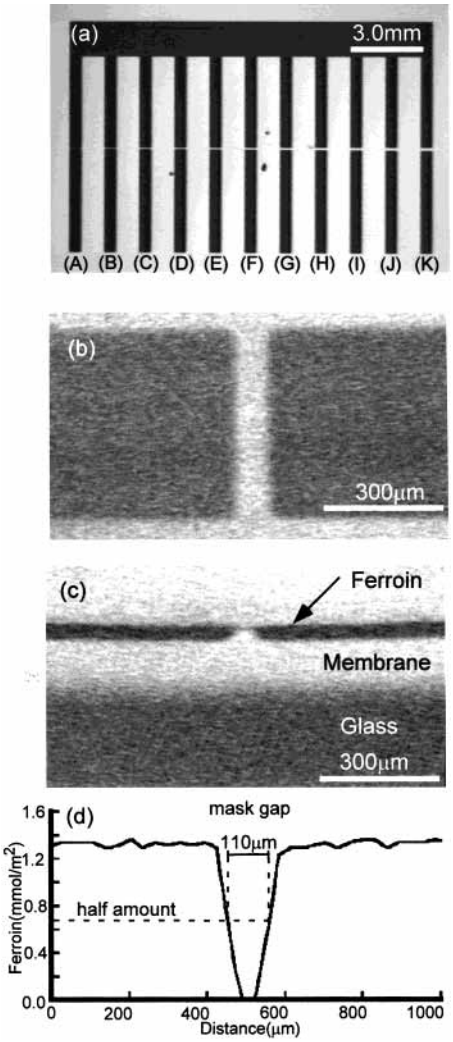

Figure 2. The catalyst (ferroin) pattern on the cation-exchange membrane (Nafion117): (a) the photograph of the whole catalyst pattern. The gaps (A)−(K) on the membrane correspond to the gap patterns on the mask with the gap widths 50, 60, 70, 80, 90, 100, 110, 120, 130, 140, and 150 μm, respectively. (b) The enlarged photograph of the gap (G). (c) The photograph of the cross section of the membrane around the gap (G). (d) The spatial distribution of the density of ferroin around the gap (G).

ferroin. The widths of the gaps on the mask, corresponding to the gaps (A)−(K), were 50−150 μm, respectively. Figure 2b shows the top view of the gap on the vertical line (G). We can see that the gap separates the black areas completely. Figure 2c shows the enlarged picture of the cross section around the gap on the vertical line (G) taken by an optical microscope. The regions with ferroin have a depth of about 35 μm. Figure 2d shows the spatial distribution of the density of ferroin (i.e., the amount of ferroin per unit area) around the gap on the vertical line (G). To estimate the amount of ferroin, we prepared standard membranes uniformly loaded with various amounts of ferroin and measured the amount of ferroin in the standard membranes by an UV−VIS spectrometer (HITACHI U-3410). Comparing the brightness of the CCD image of the patterned membrane to that of standard membranes, the amount of ferroin in the patterned membrane was estimated. Spreading of the ferroin molecules near the edge of the catalyst pattern is observed. This is probably due to the process of photoresist removal by ethanol. In this paper, we use the gap width on the mask to represent the gap width on the catalyst pattern. The actual gap width on the catalyst pattern, defined as the distance between two points where the density of ferroin becomes half that in the catalyst line, did not differ from the gap width on the mask by more than 5 μm.

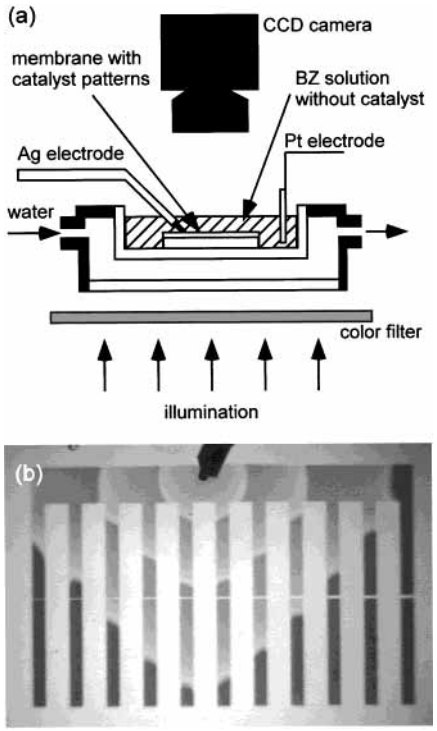

Figure 3. (a) Schematic illustration of the side view of the experimental setup and (b) photograph of chemical waves propagating along the catalyst pattern.

Experimental Setup. Figure 3a shows the configuration of our experiment. The patterned membrane on a glass plate is immersed in the BZ solution without catalyst: $[H_2SO_4] = 0.50$ M, $[NaBrO_3] = 0.4$ M, $[CH_2(COOH)_2] = 0.4$ M, $[NaBr] = 0.08$ M. The depth of the solution is about 10 mm, and the temperature of the solution is maintained at 25.0 ± 0.5 °C by a constant flow of 24.5 °C water through the heat bath. In this solution, the catalyst patterns on a membrane worked as excitable media and the chemical wave never appeared spontaneously. The catalyst pattern is red in the solution, and the front of the chemical waves is pale blue. Both the upper and the lower walls of the heat bath are made of transparent glass plates, so that the membrane can be illuminated by the light of a halogen lamp from the bottom through a blue filter (50% transmission at 441 nm). The changes between red and blue

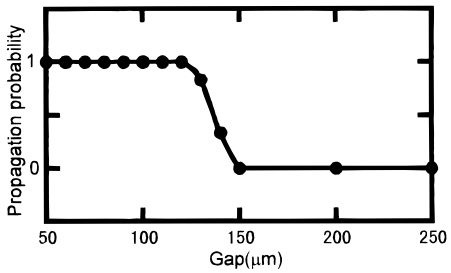

Figure 4. Dependence of the propagation probability of the chemical waves on the gap width.

were recorded as the change in the light intensity by a black-and-white CCD camera (Sony XC-77) connected to a video cassette recorder.

Initiation of the Chemical Waves. Three different methods were used to initiate chemical waves. To initiate a single chemical wave, a single circular wave was generated by touching the center of the horizontal line of the catalyst pattern with a silver wire. To initiate a periodic train of chemical waves, a spiral wave was generated near the center of the horizontal line of the catalyst pattern. The spiral offered a periodic train of chemical waves with an almost constant interval of 37 s. To initiate periodic trains of chemical waves with various periods, circular waves were periodically generated near the center of the horizontal line by an electrochemical method, which is similar to that described by Toth, Gaspar, and Showalter.[15] A silver wire electrode negatively biased at −1.25 V with respect to a platinum wire electrode in the solution was kept touching the horizontal line of the catalyst pattern. The silver wire was then negatively biased at −0.74 V for 3 s to generate a circular wave. Circular waves were periodically generated at a desired interval using a potentiostat (Nikko Keisoku NPGS-2501) triggered by a function generator (NF Electronic Instruments 1915). Figure 3b shows the chemical waves generated by the electrochemical method. Chemical waves propagate along the catalyst pattern and reach the gaps.

Results and Discussion

The Critical Gap Width and the Time Delay. The membrane with the ferroin pattern was immersed in the BZ solution without catalyst. Twenty minutes later, a single chemical wave was initiated near the center of the horizontal line of the catalyst pattern using a silver wire. The chemical wave propagated along the horizontal line and was delivered to the 11 vertical lines extending from the horizontal line. Each experiment was carried out after an interval longer than 20 min, which is long enough for the BZ reaction media on the membrane to recover its excitability.

For gap widths smaller than 130 μm the chemical waves successfully propagated through the gaps every time. For gap widths from 130 to 140 μm, the chemical waves often failed to propagate through the gaps. For gaps larger than 140 μm the chemical waves never propagated through the gaps. Figure 4 shows the dependence of the propagation probability of the chemical waves on the gap width. We can see a critical gap width (150 μm), above which no chemical waves propagate through. This phenomenon is commonly observed in BZ reaction media with a catalyst-less zone.[18−19,21]

We measured the time delay, during which a chemical wave propagates through the gap. Figure 5 shows a diagram to measure the time delay.[23] The spatial distribution of the light intensity measured along the center of a vertical line of the comb pattern is represented along the vertical axis, and the horizontal axis corresponds to the time. The diagonal white line corresponds to the locus of a chemical wave, and the horizontal white line corresponds to the position of the gap. The time delay of the propagation through the gap is defined as the length of T_d in the diagram. The values of T_d for the gap widths from 50 to 140 μm were measured.

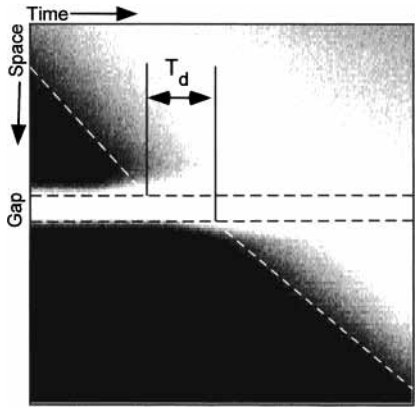

Figure 5. The space−time presentation of the chemical wave propagation.

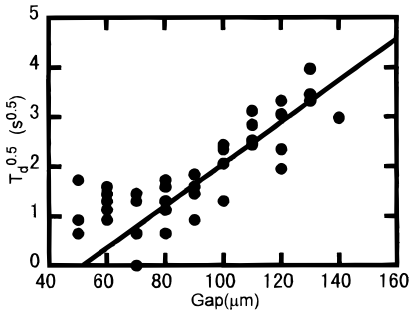

Figure 6. Dependence of the square root of T_d on the gap width.

In general, the time τ needed for the diffusion over a distance d is proportional to d^2/D, where D is the diffusion coefficient. In Figure 6, the square root of the time delay $T_d^{0.5}$ is plotted versus the gap width. For gap widths greater than 70 μm, all data points are approximately on a straight line. Thus, the diffusion of chemical species is considered to be the dominant process for these gap widths. The most probable candidate for the chemical species that carry the chemical wave through the gap is bromous acid $HBrO_2$, which is the essential autocatalyst of the BZ reaction and works as the activator of the BZ reaction.[10] For gap widths smaller than 70 μm, the data points deviate from the straight line. This might be due to the fuzziness of the edge of the catalyst pattern as shown in Figure 1d.

Frequency Change of Chemical Waves. In the previous section, propagation of a single chemical wave through the microgap was considered. In this section, we consider the propagation of periodic trains of chemical waves through the microgap. The membrane with ferroin pattern was immersed in the BZ solution without catalyst. Twenty minutes later, a periodic train of chemical waves was initiated by the spiral wave or by the electrochemical method described in the Experimental Section. Figure 7 shows the photograph of the periodic train of chemical waves propagating from a spiral center near the center of the horizontal line of the comb pattern. The white bands on the catalyst pattern correspond to the regions of the chemical waves. The firing number[15,25,26] N_f (defined as the ratio of the number of chemical waves that successfully propagate through the gap to the number of chemical waves that enter the gap) is plotted versus the gap width in Figure 8. For gap widths smaller

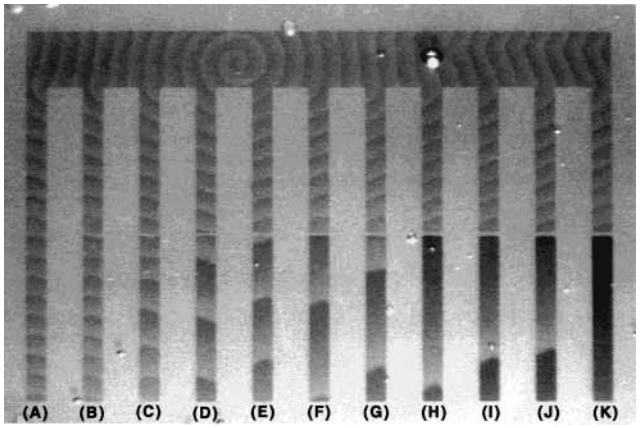

Figure 7. Photograph of the spiral wave propagating along the comb pattern.

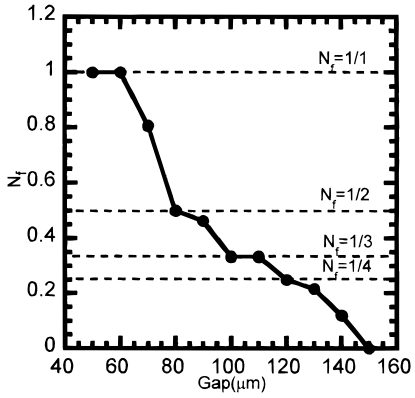

Figure 8. Dependence of the firing number N_f on the gap width.

than 70 μm (50 (A) and 60 μm (B)), all the waves propagated through the gap. On the other hand, no waves propagated through the 150 μm gap (A). For gap widths between 70 (C) and 140 μm (J), propagation failures of chemical waves occurred depending on the gap width. For particular gap widths (80 (D), 100 (F), 110 (G), and 120 μm (H)), the propagation failure occurred periodically. N_f can be represented by $N_f = 1/n$ (n = 1, 2, 3, 4) for these gaps. For intermediate gap widths between these particular gap widths, propagation failures occurred aperiodically. An aperiodic propagation failure is likely to be a random combination of the adjacent two periodic propagation failures. For these intermediate gap widths, the experimental noise might disturb the periodic propagation.

The time variations of the intensity of the brightness at the upper and lower sides of the gaps (A), (D), (F), and (H) observed by the CCD camera are shown in Figure 9. For gap (A), every wave propagated through the gap. For the gaps (D), (F) and (H), one wave in every two, three, and four waves propagated through the gap, respectively. In this way, the frequency of the chemical waves was converted into lower frequencies, such as $^1/_2$, $^1/_3$, and $^1/_4$ of the original frequency. Each of the frequency changes lasted at least for 30 min despite the gradual compositional change of the BZ solution.

To investigate the dependence of the frequency change on the original period T_{in} of the chemical waves entering the gaps, periodic trains of chemical waves with various periods were initiated at the center of horizontal line of the catalyst pattern using the electrochemical method described in the Experimental Section. The result is summarized in Figure 10, in which periodic propagation is classified by firing number $N_f = 0$, 1/n (n = 1, 2, 3, 4). For each gap width, N_f becomes smaller as T_{in}

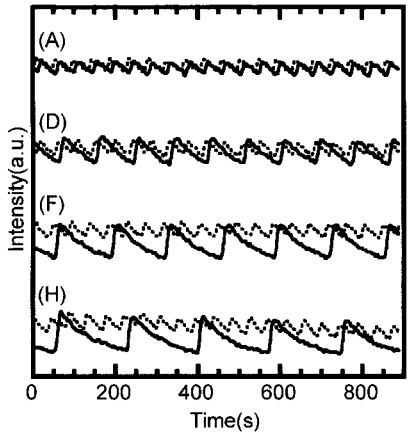

Figure 9. Time variations of the brightness observed by the CCD camera at both the upper and lower sides of the gaps (A), (D), (F), and (H). The dotted lines and the solid lines represent the time variation of the brightness at the upper and lower sides, respectively.

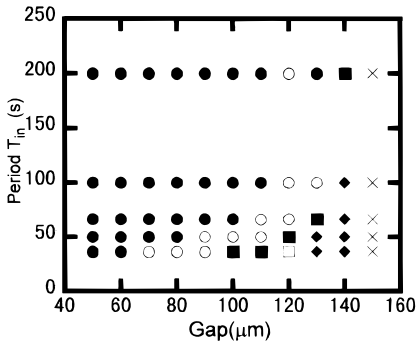

Figure 10. Diagram of the chemical wave propagation versus the gap width and the period T_{in} of chemical waves entering the gap. The firing number N_f is indicated by ● ($1/1 \le N_f < 1/1.5$), ○ ($1/1.5 \le N_f < 1/2.5$), ■ ($1/2.5 \le N_f < 1/3.5$), □ ($1/3.5 \le N_f < 1/4.5$), ◆ ($1/4.5 \le N_f$), × (no propagation).

becomes shorter. The critical period $T_c(n)$ can be defined for each firing number $N_f = 1/n$ (n = 1, 2, 3, 4)), as the value of T_{in} at which N_f decreases from $1/n$ to $1/(n + 1)$. $T_c(n)$ values are discussed below.

The frequency change of chemical waves mentioned above is a result of the propagation failures of chemical waves at the gap. The propagation failures can be explained on the basis of a simplified picture based on the concept of refractoriness.[14,27] That means the success or failure of the chemical wave propagation can be explained by the next conditions:

If $T_{rest} > T_r$ then the propagation occurs.

If $T_{rest} < T_r$ then the propagation fails.

Here T_{rest} is the time elapsed since the last excitation at the lower side of the gap before the next chemical wave enters the gap. T_r is the recovery time (or refractory period) during which the BZ reaction medium at the lower side of the gap recovers its excitability sufficiently to be excited by $HBrO_2$ diffusing from the upper side of the gap.

For $T_{in} \ge T_r$, each chemical wave arrives at the lower side of the gap after the excitability is recovered. In this case, all the chemical waves successfully propagate through the gap, and therefore, $N_f = 1$. For a smaller value of T_{in}, the excitability does not recover before the arrival of the second wave. For $T_{in} < T_r \le 2T_{in}$, the excitability recovers between the arrivals of the second and the third waves, allowing only the third wave to propagate. In this case, one wave in every 2 waves successfully propagates and $N_f = 2$. Similarly $N_f = 3$ for $2T_{in} < T_r \le 3T_{in}$. In this way, the change of N_f depending on T_{in}

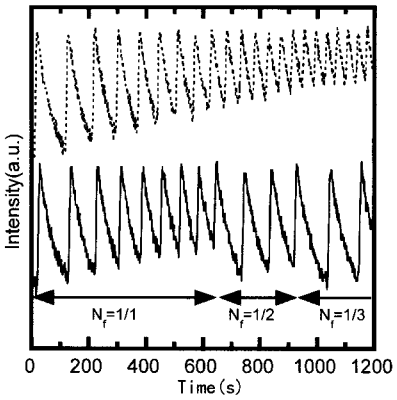

Figure 11. Time variations of the brightness observed by the CCD camera at both the upper and lower sides of the gap (E), when the period of chemical waves entering the gaps was gradually reduced. The dotted line and the solid line represent the time variation of the brightness at the upper and lower sides of the gap (E), respectively.

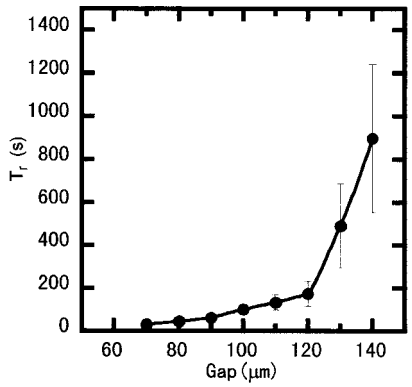

Figure 12. Dependence of the recovery time T_r on the gap width.

can be explained by the simplified picture of the chemical wave propagation. In this picture, the critical periods $T_c(1)$, $T_c(2)$, $T_c(3)$ are given by T_r, $T_r/2$, $T_r/3$, respectively.

In the simplified picture of the chemical wave propagation, T_r plays an important role. To measure T_r precisely, T_{in} was gradually reduced. An example of the time variation of the brightness at the upper and lower sides of the gap (E) observed by the CCD camera is indicated by the dotted and solid lines in Figure 11, respectively. In the early stage, T_{in} was long and all waves successfully propagated through the gap. As T_{in} became smaller, the changes of N_f took place one after another.

In Figure 11, T_r corresponds to the minimum period of the chemical waves observed at the lower side of the gap immediately before the change of N_f from 1 to $^1/_2$. T_r is plotted versus the gap width in Figure 12. This curve corresponds to the boundary between the region of $N_f = 1$ and the region of $N_f = {}^1/_2$ in Figure 10. T_r rapidly increases with increasing gap width. This is the origin of the frequency change depending on the gap width. The dependence of T_r on the gap width can be explained as follows. As the gap width increases, the amount of $HBrO_2$ reaching the lower side of the gap becomes smaller. Therefore the medium needs more time to recover its excitability sufficiently to be excited by the smaller amount of $HBrO_2$. This is a characteristic feature of excitable media in a relative refractory period (i.e., a period during which the excitability of an excitable media is recovering, and the strength of the stimulation which can cause the excitation of the system is depending on the excitability.).

Next, we consider the change of T_r for a constant gap width. The minimum periods of the chemical waves observed at the lower side of the gap immediately before the changes of N_f from $1/n$ to $1/(n+1)$ ($n = 1, 2, 3$) correspond to the values of T_r. In other word, the values of T_r are given by $T_c(1)$, $2T_c(2)$, and $3T_c(3)$, respectively. These values are plotted versus the number n in Figure 13. T_r increases with the number n. For the gap width of 110 μm, the change of T_r is about 10%. For the gap width of 90 μm, $3T_c(3)$ is almost twice as large as $T_c(1)$.

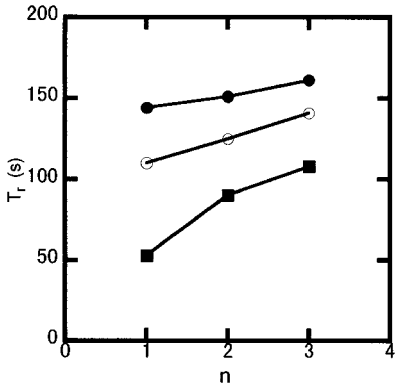

Figure 13. Dependence of the recovery time T_r on the number n ($N_f = 1/n$). T_r is indicated by ● (110 μm), ○ (100 μm), ■ (90 μm).

One possible reason for the increase of T_r is that the amplitude of the chemical waves entering the gap decreases with the period of the chemical waves, as shown in Figures 9 and 11. The decrease of the amplitude results in the decrease of the amount of $HBrO_2$ released from the upper side of the gap. Accordingly, the amount of $HBrO_2$ reaching the lower side of the gap becomes smaller. As a result, the medium needs more time to recover its excitability sufficiently to be excited by the smaller amount of $HBrO_2$. In addition, Finkenová, Dolnik, Hrudka, Schreiber, and Mareck have thoroughly investigated periodically stimulated excitable BZ reaction in CSTR and have obtained the phase-excitation curves (PEC's).[25,26] According to their reports, even the stimulation which fails to induce the excitation of the BZ reaction can cause the negative phase shift (i.e., a lengthening of the actual refractory period) of the excitation cycle of the BZ reaction system. In our system, similar phase shifts might have occurred. In other words, even chemical waves that failed to propagate through a gap might be able to shift the phase of the excitation cycle of a BZ reaction medium at the lower side of the gap negatively and make the actual T_r longer.

Very similar frequency changes of the chemical waves have been observed in different systems. Tóth et al. have reported the frequency change of the chemical waves propagating through narrow capillary tubes, where the high curvatures of the wave front caused the frequency change.[15] In addition, Oosawa et al. have reported the frequency change of the chemical wave propagating through a boundary between two BZ media made by different sizes of cation-exchange beads, where the difference in the refractory periods between the two BZ media caused the frequency change.[9] In our system, the frequency change of the chemical waves is caused by the dilution of $HBrO_2$ due to its diffusion through the microgap.

Changes of Wave Velocities. As shown in Figure 14, changes of wave velocity occurred subsequent to the frequency changes of the chemical waves. This change of wave velocity can be explained in terms of a dispersion relation of chemical waves. The dispersion relation of chemical waves propagating on our catalyst patterns on the membrane is shown in Figure 15. For higher frequencies, the amplitude of oscillation becomes smaller and the wave velocity becomes lower. In the same figure, the wave velocities observed under the gaps (A), (D),

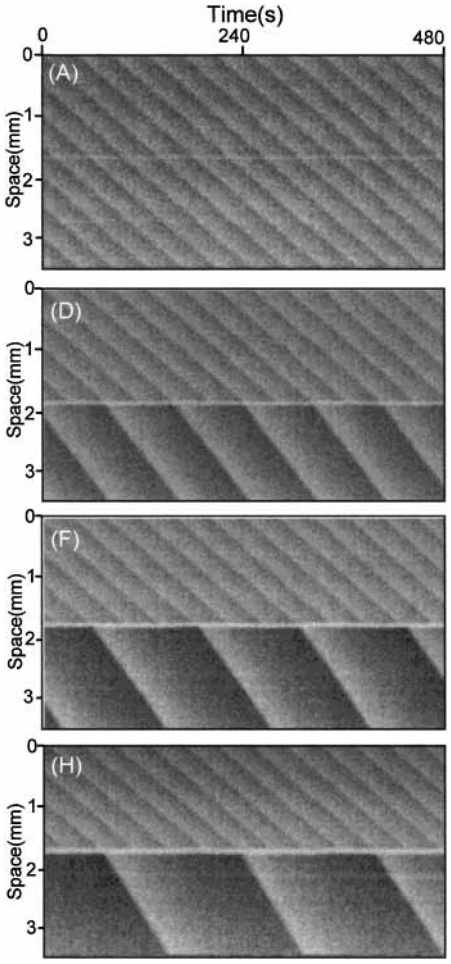

Figure 14. The space−time diagrams of the propagation of chemical waves around the gaps (A), (D), (F), and (H), respectively. The spatial distributions of the brightness measured along the centers of corresponding vertical lines are represented along the vertical axis, and the horizontal axis corresponds to the time. The diagonal white lines correspond to the loci of the chemical waves, and the horizontal white lines correspond to the position of the gaps.

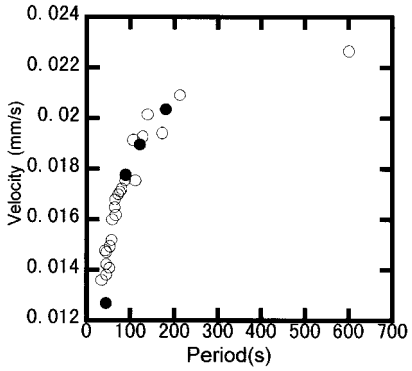

Figure 15. Dispersion relation of the chemical waves on the membrane and the wave velocities observed on the lines under the gaps (A), (D), (F), and (H). The dispersion relation is indicated by (○). The velocities of waves under the gaps are indicated by (●).

(F), and (H) are plotted. It is clear that these wave velocities agree with the curve of the dispersion relation. Thus the change of the wave velocity can be explained completely in terms of the dispersion relation of chemical waves. The change of wave velocity makes the wavelength under the gaps (D), (F), and (H) larger than 2, 3, and 4 times the original wavelength as shown in Figure 7.

Conclusions

The chemical wave propagation through the microgaps of the catalyst pattern was investigated. For a single chemical wave, there was a critical gap width above which no propagation through the gap was possible. The dependence of the time delay on the gap width suggested that the chemical waves propagate through the gap via mass diffusion. For a periodic train of chemical waves, the frequency conversion was observed at the gap depending on the gap width and the original frequency. The frequency change can be explained in terms of the recovery time of the BZ reaction media. The propagation failures of chemical waves can be explained consistently with all the experimental results.

Finally, the present results suggest that the spatial resolution of the catalyst pattering technique is comparable with the diffusion length in the BZ reaction media. Therefore it would be possible to construct an arbitrary micropattern precisely enough to control the propagation of chemical waves. Thus, various chemical-based computational devices[19,21−23] to explore the possibilities for information processing can be realized by this technique.

References and Notes

(1) Zaikin, A. N.; Zhabotinsky, A. M. *Nature* **1970**, *225*, 535.

(2) Winfree, A. T. *Science* **1972**, *175*, 634.

(3) Field, R. J., Burger, M., Eds. *Oscillation and Traveling Waves in Chemical Systems*; Wiley: New York, 1984.

(4) Kapral, R., Showalter, K., Eds. *Chemical Waves and Patterns*; Kluwer: Dordrecht, The Netherlands, 1995.

(5) Scott, S. K. *Oscillations, Waves, and Chaos in Chemical Kinetics*; Oxford University Press: Oxford, 1994.

(6) Swinney, H. L.; Krinsky, V. I., Eds. *Waves and Patterns in Chemical and Biological Media*; MIT Press: Cambridge, 1992.

(7) Maselko, J.; Showalter, K. *Nature* **1989**, *339*, 609.

(8) Maselko, J.; Reckley, J. S.; Showalter, K. *J. Phys. Chem.* **1989**, *93*, 2774.

(9) Oosawa, C.; Fukuta, Y.; Natsume, K.; Kometani, K. *J. Phys. Chem.* **1996**, *100*, 1043.

(10) Steinbock, O.; Kettunen, P.; Showalter, K. *Science* **1995**, *269*, 1857.

(11) Steinbock, O.; Zykov, V. S.; Müller, S. C. *Phys. Rev. E* **1993**, *48*, 3295.

(12) Zhabotionsky, A. M.; Eager, M. D.; Epstein, I. R. *Phys. Rev. Lett.* **1993**, *71*, 1526.

(13) Zhabotinsky, A. M.; Györgyi, L.; Dolnik, M.; Epstein, I. R. *J. Phys. Chem.* **1994**, *98*, 7981.

(14) Volford, A.; Noszticzius, Z.; Krinsky, V.; Dupont, C.; Lázár, A.; Försterling, H. D. *J. Phys. Chem. A* **1998**, *102*, 8355.

(15) Tóth, Á.; Gáspár, V.; Showalter, K. *J. Phys. Chem.* **1994**, *98*, 522.

(16) Tóth, Á.; Showalter, K. *J. Chem. Phys.* **1995**, *103*, 2058.

(17) DeSimone, J. A.; Beil, D. L.; Scriven, L. E. *Nature* **1973**, *180*, 946.

(18) Linde, H.; Zirkel, C. *Z. Phys. Chem.* **1991**, *174*, 145.

(19) Agladze, K.; Dupont, C.; Krinsky, V. *Nuovo Cimento D* **1998**, *20D*, 103.

(20) Zipes, D. P., Jalife, J., Eds. Cardiac *Electrophysiology: From Cell to Bedside*; Saunders: Philadelphia, 1995.

(21) Steinbock, O.; Kettunen, P.; Showalter, K. *J. Phys. Chem.* **1996**, *100*, 18970.

(22) Agladze, K.; Aliev, R. R.; Yamaguchi, T.; Yoshikawa, K. *J. Phys. Chem.* **1996**, *100*, 13895.

(23) Kusumi, T.; Yamaguchi, T.; Aliev, R. R.; Amemiya, T.; Ohmori, T.; Hashimoto, H.; Yoshikawa, K. *Chem. Phys. Lett.* **1997**, *355*, 271.

(24) Suzuki, K.; Yoshinobu, T.; Iwasaki, H. *Jpn. J. Appl. Phys.* **1999**, *38*, L345.

(25) Dolnik, M.; Finkenová, J.; Schreiber, I.; Marek, M. *J. Phys. Chem.* **1989**, *93*, 2764.

(26) Finkeová, J.; Dolnik, M.; Hrudka, B.; Marek, M. *J. Phys. Chem.* **1990**, *94*, 4110.

(27) Krinsky, V. I. *Biofizika* **1996**, *11*, 676.